

SOLUTION OF DENDRITIC GROWTH IN A BINARY ALLOY BY A NOVEL POINT AUTOMATA METHOD

A.Z. LORBIECKA* AND B. ŠARLER†

* University of Nova Gorica
Vipavska 13, Rožna Dolina
Nova Gorica, Slovenia
e-mail: alorbiecka@ung.si

† University of Nova Gorica
Vipavska 13, Rožna Dolina
Nova Gorica, Slovenia
email: bozidar.sarler@ung.si

Key words: Cellular Automata (CA), Point Automata (PA), Dendritic Growth, Heat and Mass Transfer.

Abstract. The aim of this paper is simulation of thermally induced liquid-solid dendritic growth in a binary alloy (Fe-0.6%C) steel in two dimensions by a coupled deterministic continuum mechanics heat and species transfer model and a stochastic localized phase change kinetics model that takes into account the undercooling, curvature, kinetic, and thermodynamic anisotropy. The stochastic model receives temperature and concentration information from the deterministic model and the deterministic heat and species diffusion equations receive the solid fraction information from the stochastic model. The heat and species transfer models are solved on a regular grid by the standard explicit Finite Difference Method (FDM). The phase-change kinetics model is solved by the novel Point Automata (PA) approach. The PA method was developed and introduced [1,2] in order to circumvent the mesh anisotropy problem, associated with the classical Cellular Automata (CA) method. Dendritic structures are in the CA approach sensitive on the relative angle between the cell structure and the preferential crystal growth direction which is not physical. The CA approach used in the paper for reference comparison is established on quadratic cells and Neumann neighborhood. The PA approach is established on randomly distributed points and neighborhood configuration, similar as appears in meshless methods. Both methods provide same results in case of regular PA node arrangements and neighborhood configuration with five points. A comparison between both stochastic approaches has been made with respect to dendritic growth with different orientations of crystallographic angles. It is demonstrated that the new PA method can cope with dendritic growth of a binary alloy in any direction which is not the case with the CA method.

1 INTRODUCTION

Numerical modeling is having an increasingly important role in studies of dendritic growth

during solidification [3]. The simulation of microstructure based on the CA technique can reproduce most of the dendritic features observed experimentally with the acceptable computational efficiency. However, simple CA models are not capable of reproducing the typical growth features of dendrites when the primary branches do not coincide with the preferential mesh orientations. The reason for that is that the simple CA models suffer from the strong impact of the mesh orientation. It does not matter which crystallographic orientation will be chosen, the CA will always shift the dendrite with respect to the grid axis. The crystallographic orientation axes of different dendrites have in general different angles with respect to the coordinate system. We use a novel Point Automata (PA) method in this paper. It follows the CA concept and is able to solve the mentioned crystallographic orientation problem. A basic feature of this method is the random distribution of the nodes in the domain instead of using regular cells, which leads to different distances between the nodes and different neighborhood configurations for each of them. This new concept was first proposed by Janssens for modeling the recrystallization [4,5]. The first results of the dendritic growth with various orientations based on the PA method have been developed in [1] for pure metals. The PA algorithm, developed in the present paper, is able to obtain the dendritic morphology of solidifying binary alloy (Fe-0.6% C steel is taken as an example), by solving the heat and mass transfer equations, coupled with the solid fraction field through the calculations of the crystal growth velocity, interface curvature, thermodynamic and kinetic anisotropy, respectively. Previous classical CA solutions of the dendritic growth of the Fe-0.6% C steel are demonstrated in [6,7]. The present paper is structured in the following way: the governing equations of the heat and mass transfer model are defined first, followed by the description of the stochastic model. The solution of temperature, concentration field and solid fraction is explained afterwards. Finally, the numerical results of FDM-PA method are shown and compared with the results of the FDM-CA method.

2 MODEL DESCRIPTION

Consider a two dimensional domain Ω with boundary Γ filled with a binary phase change material which consists of at least two phases, solid and liquid, separated by an interfacial region.

2.1 Heat and species transport

2.1.1 Heat diffusion

The following heat transport equation is solved first:

$$\frac{\partial}{\partial t}(\rho h) = \nabla \cdot (\lambda \nabla T) \quad (1)$$

where ρ , h , λ , T represent material density, specific enthalpy, thermal conductivity and temperature, respectively. The specific enthalpy is constituted as $h = c_p T + f_l L$, where c_p , L , f_l represent the specific heat, the latent heat and liquid fraction, respectively. All material

properties are assumed constant for simulation simplicity. We search for the temperature at time $t_0 + \Delta t$ by assuming the initial conditions:

$$T(\mathbf{p}, t_0) = T_0(\mathbf{p}); \mathbf{p} \in \Omega; f_s(\mathbf{p}, t_0) = f_{s0}(\mathbf{p}); \mathbf{p} \in \Omega \quad (2)$$

(where \mathbf{p} represents the position vector) and Neumann boundary conditions:

$$\frac{\partial T}{\partial \mathbf{n}}(\mathbf{p}, t) = F(\mathbf{p}, t); \mathbf{p} \in \Gamma, t_0 < t \leq t_0 + \Delta t \quad (3)$$

where \mathbf{n} represents the normal on Γ and T_0, f_{s0}, F represent known function.

2.1.2 Species diffusion

The solution of the heat transfer equation is followed by the solution of the solute transfer equation. The governing equation for the solute transfer in both solid and liquid phases is formulated in terms of mixture concentration [8]:

$$c = f_s c_s + (1 - f_s) c_l \quad (4)$$

$$\frac{\partial c}{\partial t} = \nabla \cdot (D \nabla c) - c(1 - k_p) \frac{\partial f_s}{\partial t} \quad (5)$$

where D stands for solute diffusion coefficient, defined as $D = f_s D_s + (1 - f_s) D_l$ with D_s and D_l defining the solute diffusion coefficients in solid and liquid, respectively. It is assumed that the concentrations of solid and liquid at the interface are in equilibrium i.e. $c_s = k_p c_l$ where k_p, c_s and c_l are the partition coefficient, concentration in the solid and liquid phase, respectively. We search for the concentration c at time $t_0 + \Delta t$ by assuming the initial and Neumann boundary conditions:

$$c(\mathbf{p}, t_0) = c_0(\mathbf{p}); \mathbf{p} \in \Omega \quad (6)$$

$$\frac{\partial c}{\partial \mathbf{n}}(\mathbf{p}, t) = F(\mathbf{p}, t); \mathbf{p} \in \Gamma, t_0 < t \leq t_0 + \Delta t \quad (7)$$

2.2 Solid fraction calculations

2.2.1 Interface undercooling

The phase change situation can be achieved by undercooling a liquid below its liquid temperature. When a solid seed is placed in such an undercooled melt, solidification will be initiated. Due to crystal anisotropy and perturbations in the system, the growth of the solid

from the seed will not be uniform and an equiaxed dendritic crystal will form. The solid liquid interface is undercooled to the temperature T_f defined as [9]:

$$T_f = T_l + m(c_l - c_0) - \Gamma K \quad (8)$$

where Γ , K , m are the Gibbs-Thomson coefficient, the interface curvature and the liquidus slope, respectively.

2.2.2 Growth velocity

The growth process is driven by the local undercooling. The interface growth velocity is given by the classical sharp model [10]:

$$V_g^*(\mathbf{p}, t) = \mu_K (T_f - T(\mathbf{p}, t)); \mathbf{p} \in \Gamma_{s,l} \quad (9)$$

where V_g^* , μ_K , $\Gamma_{s,l}$ are the growth velocity, interface kinetics coefficient and the solid liquid interface, respectively. Dendrites always grow in the specific crystallographic orientations. Therefore it is necessary to consider anisotropy in either the interfacial kinetics or surface energy (or both). The present model accounts for the anisotropy in both kinetics.

2.2.3 Thermodynamic anisotropy

The Gibbs-Thomson coefficient can be evaluated by taking into account the thermodynamic anisotropy related to the crystal orientation and type as follows:

$$\Gamma = \bar{\Gamma} \left[1 - \delta_t \cos \left[S(\theta - \theta_{def}) \right] \right] \quad (10)$$

where S , θ , θ_{def} , δ_t , $\bar{\Gamma}$ represent factors which control the number of preferential directions of the material's anisotropy ($S = 0$ for the isotropic case, $S = 4$ for four fold anisotropy and so on), growth angle (angle between the y coordinate and the line that connects the centre of the mass of the dendrite and point at $\Gamma_{s,l}$), the preferential crystallographic orientation, thermodynamic anisotropy coefficient and the average Gibbs-Thomson coefficient, respectively.

2.2.4 Kinetic anisotropy

The crystal growth velocity is calculated according to the crystal orientation by taking into the consideration the crystal growth direction θ and the preferred orientation θ_{def} . The crystal growth velocity follows:

$$V = V_g^*(\mathbf{p}, t) \left[1 + \delta_k \cos \left(S(\theta - \theta_{def}) \right) \right] \quad (11)$$

where δ_k represents the degree of the kinetic anisotropy.

3 COUPLING

The represented numerical model consists of two schemes: FDM for evaluating the heat and mass transport (Section 2.1) and a novel PA method for simulating the phase change kinetics (Section 2.2). The calculation domain is divided into FDM nodes used for the calculation of the temperature and solute profiles and random PA points to calculate the solid fraction field. Each four regularly spaced FDM nodes include one random point between them (or a CA cell located in the center between them), see Figure 1. The number of points in FDM mesh in x and y directions is N . At one time step, heat and solute fields are first calculated for the FDM nodes. These values need to be interpolated from the FDM nodes to PA points (or CA cells in case of the CA method). Then, based on the obtained profiles, the local undercooling and the growth velocity of the interface are calculated using Equations 8 and 9. Afterwards, a new solid fraction f_s for PA points (or CA cells in case of CA method) is calculated. At the end of the time step are the temperature field and solute field are updated, based on the new solid fraction profile. The procedure is repeated in the next time step by using the calculated temperature, concentration, and solid fraction fields as initial data.

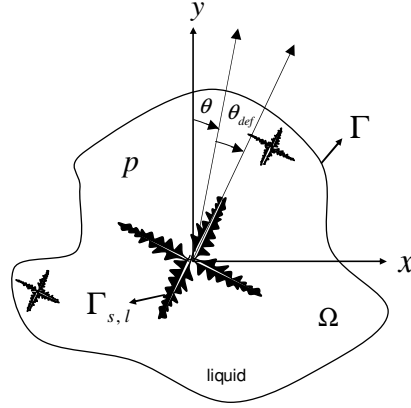


Figure 1: Scheme of the dendritic growth

3.1 Solution of temperature and concentration field

The solution of the temperature field is performed by the simple explicit FDM scheme through the following discretised equation:

$$T_{i,j} = T_{0i,j} + \frac{\Delta t \lambda}{\rho c_p} \left(\left[(T_{0i-1,j} - 2T_{0i,j} + T_{0i+1,j}) / (\Delta x^2) \right] + \left[(T_{0i,j-1} - 2T_{0i,j} + T_{0i,j+1}) / (\Delta y^2) \right] + \frac{L}{c_p} (f_{s i,j} - f_{0s i,j}) \right) \quad (12)$$

for $i = 2, 3, \dots, N-1$ and $j = 2, 3, \dots, N-1$, where Δt , $f_{0s i,j}$, $T_{0i,j}$, $T_{0i+1,j}$, $T_{0i-1,j}$, $T_{0i,j+1}$, $T_{0i,j-1}$, ρ , h , λ represent the time step, initial solid fraction, initial temperature in the FDM central, east, west, north and south nodes, material density, specific enthalpy and thermal conductivity, respectively. The solution of the concentration field is performed by the simple explicit FDM scheme through the following discretised equation:

$$c_{i,j} = c_{0i,j} + \Delta t D \left[\left(c_{0i-1,j} - 2c_{0i,j} + c_{0i+1,j} \right) / (\Delta x^2) \right] + \left[\left(c_{0i,j-1} - 2c_{0i,j} + c_{0i,j+1} \right) / (\Delta y^2) \right] - c_{0i,j} \left[(1-k_p)(f_{si,j} - f_{0si,j}) \right] \quad (13)$$

for $i = 2, 3, \dots, N-1$ and $j = 2, 3, \dots, N-1$, where Δt , $f_{0si,j}$, $c_{0i,j}$, $c_{0i+1,j}$, $c_{0i-1,j}$, $c_{0i,j+1}$, $c_{0i,j-1}$ are the time step, initial solid fraction, initial concentration in the FDM central, east, west, north and south nodes, respectively. The obtained values of concentration on regular FDM grid are in each time step transferred to random PA grid (or regular CA grid). The rejected solute amount $\Delta c = c_l - k_p c_l$ is added to the liquid points in the surrounding neighbors which fall into the circle of $R_{C-H} = 20a$, where a represents the typical mesh distance for each cell (point) separately. Thus, the overall solute in the domain can be kept consistent. A detailed description of FDM-PA (FDM-CA) transfer of temperature and PA-FDM (CA-FDM) transfer of solid fraction from the regular to the random grids and vice versa is elaborated in [1]. The same algorithms are used in the present paper.

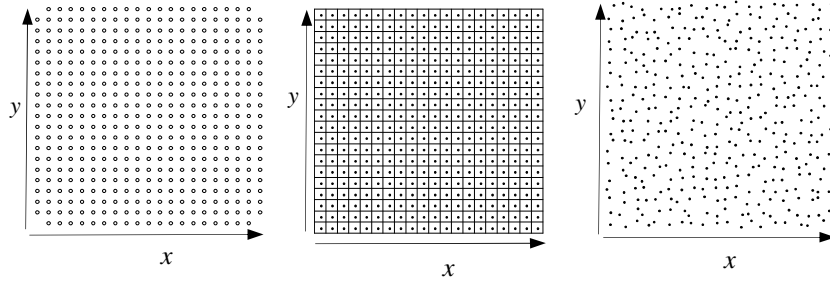


Figure 2: Scheme of space discretization: (left) FDM nodes with $N = 21$, (middle), CA cells with $n = 20$, (right) PA nodes with $n = 20$

3.2 Interface curvature calculations

The interface curvature is approximated by the counting cell procedure developed by Sasikumar and Sreenivasan [11]. The expression for PA is derived from the expression of the CA method by assuming the average node distance \bar{a} instead of the regular node distance a .

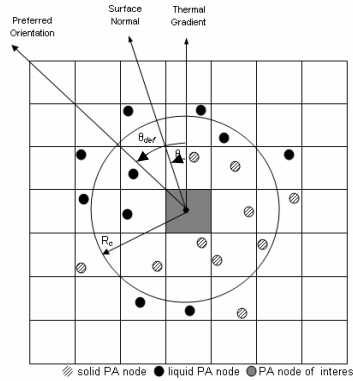


Figure 3: A scheme of curvature calculation in the PA method with $R_c = 2a$ (example with: $N_{sPA} = 7$ and $N_{lPA} = 11$)

The expression for curvature K is given by the formula:

$$K = \frac{1}{a} \left(1 - \frac{2N_{sPA}}{N_{tPA}} \right) \quad (14)$$

where N_{sPA} and N_{tPA} are the number of random points whose centres fall inside the circle of assumed radius R_c and the total number of points whose centres fall inside the circle, respectively.

Some fluctuations need to be introduced into the calculations in order to avoid the symmetric shape of the dendrite in the conventional CA approach. Thermal noises are usually presented by putting the random fluctuations into the calculations of latent heat, undercooling temperature or velocity [12]. In the present study it is not necessary to put any thermal fluctuations in the PA method. The random node arrangements in the PA method replace the thermal fluctuations of the CA method.

In the CA approach only the closest, Moore neighbourhood configuration [3] has been analysed. In the PA method, solid grows with respect to the ‘neighbourhood’ configuration which is now associated with the position of the neighbouring PA nodes which fall into a circle with radius R_H [2]. The radius of neighbourhood should be kept at a minimum of 1.5 μm in case of $a = 0.5 \mu\text{m}$. For smaller values the dendritic shapes become distorted and the preferred orientations are lost.

4 NUMERICAL EXAMPLE

4.1 Definition of test case

A dendritic growth of Fe-0.6% C steel solidifying into an undercooled melt is simulated. The square computational domain with length $350 \mu\text{m}$ is divided into 701×701 FDM nodes and 700×700 randomly located PA points. Each four FDM nodes involve one PA node (randomly located between the four FDM nodes). At the beginning of the simulation nucleus(es) is assigned with the preferential orientation(s) and start to growth with respect to above algorithm. The initial solid concentration for point is assumed to be $c_s = k_p c_0$ with temperature $T_l = 1490^\circ\text{C}$ at $c_0 = 0.6 \%$ wt. The nominal parameters used in all presented simulations are listed in Table 1. Varied data are presented in Table 2. In the numerical simulation the reference CA method has been used. The details of this method and numerical implementation are elaborated in [1].

4.2 Results

The numerical examples in the present paper are solved by the FDM based temperature and concentration calculations and PA based solid fraction calculations. Our testing was primarily focused on the growth of the dendrite at different orientations by the novel PA method coupled with the heat and mass transfer calculations. To achieve the same length for primary and secondary dendrite arms in PA method as in the CA method, an empirical factor, which

multiplies the calculated velocity in the PA method, has to be introduced. It can be shown that putting a factor of 1.25 in the growth velocity calculations for PA, the branches will have the same length in both methods. Detailed discussion of model parameters was elaborated in [1]. The following numerical examples are shown:

- Case 1 and Case 2 represent the dendritic growth process simulated for Fe-0.6% C steel for undercooling of $\Delta T = 250$ °C by the FDM-CA and FDM-PA methods. The calculation time of both methods is practically the same (Figure 5).
- From Case 3 to 4 the dendritic growth process is simulated for Fe-0.6% C steel for two different preferential orientations $\theta_{def} = 15^\circ$ and $\theta_{def} = 32^\circ$ by the FDM-PA method (Figure 6).
- Case 5 represents six dendrites growing simultaneously simulated by the FDM-PA method.
- On Figure 4 the concentration profiles along the primary dendrite arms obtained by the FDM-CA method are depicted (for Case 1). (Figure 7).

Table 1: Nominal parameters used in the calculations for Fe 0.6% C

Symbol	Value	Unit
ρ	7300	kg/m ³
T_l	1490	°C
λ	30	W/mK
c_p	800	J/kgK
L	2.7×10^{-5}	J/kg
D_s	5.0×10^{-10}	m ² /s
D_l	2.0×10^{-9}	m ² /s
c_0	0.6	%
k_p	0.34	1
Δt	7.65×10^{-10}	s
$\bar{\Gamma}$	1.9×10^{-7}	Km
δ_k	0.75	1
S	4	1
R_c	1.5	μm
R_H	2	μm
μ_K	0.2	m/sK
l	350	μm
n	700	PA nodes/ CA cells
N	701	FDM nodes

Table 2: Varied parameters in different cases

Case	Method	angle	ΔT
CASE 1	FDM-CA	$\theta_{def} = 0^\circ$	$\Delta T = 250^\circ \text{C}$
CASE 2	FDM-CA	$\theta_{def} = 0^\circ$	$\Delta T = 250^\circ \text{C}$
CASE 3	FDM-PA	$\theta_{def} = 15^\circ$	$\Delta T = 150^\circ \text{C}$
CASE 4	FDM-PA	$\theta_{def} = 32^\circ$	$\Delta T = 150^\circ \text{C}$
CASE 5	FDM-PA	$4^\circ, 14^\circ, 33^\circ, 28^\circ, 43^\circ, 8^\circ, 0^\circ$	$\Delta T = 150^\circ \text{C}$

5 CONCLUSIONS

In this paper the temperature and mass transfer equations are coupled with the novel PA method to calculate the solid fraction field in the dendritic growth. Advantages of the developed PA method are:

- No need for mesh generation or polygonisation. Only the node arrangement has to be generated, but without any geometrical connection between the nodes.
- In the new PA method is the microstructure evolution solved with respect to the location of the points (not polygons) on the computational domain.
- The random grid PA method allows rotating dendrites in any direction since it has a limited anisotropy of the node arrangements.
- PA method offers a simple and powerful approach of CA type simulations. It is shown that both methods are able to qualitatively and quantitatively model a diverse range of solidification phenomena in almost the same calculation time.
- The dimension of the neighborhood radius and generation of the random node arrangement has to be chosen carefully in order to be able to rotate the dendrite.
- Straightforward node refinement possibility.
- Straightforward extension to 3-D.

ACKNOWLEDGEMENT

This paper forms a part of the project J2-0099 Multiscale Modelling of Liquid-Solid Processes. Financial support from Slovenian Grant Agency is gratefully acknowledged.

REFERENCES

- [1] Lorbiecka, A.Z. and Šarler, B. Simulation of dendritic growth with different orientation by using the point automata method. *Computers, Materials, Continua* (2010) **18**:69-104.
- [2] Lorbiecka, A.Z. and Šarler, B. A sensitivity study of grain growth model for prediction of ECT and CET transformations in continuous casting of steel. *Materials Science Forum* (2010) **649**: 373-378.

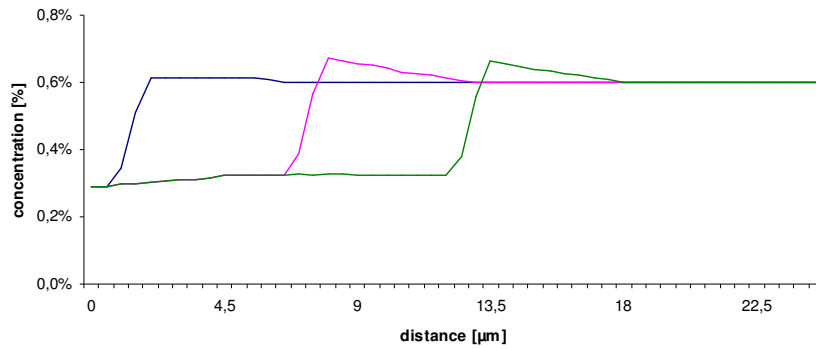


Figure 4: Concentration profiles along the primary dendrites arms obtained by the FDM-PA method for different solidification time: 0.15×10^{-6} [s] (blue line), 1.37×10^{-6} [s] (pink line) and 2.4×10^{-6} [s] (green line)

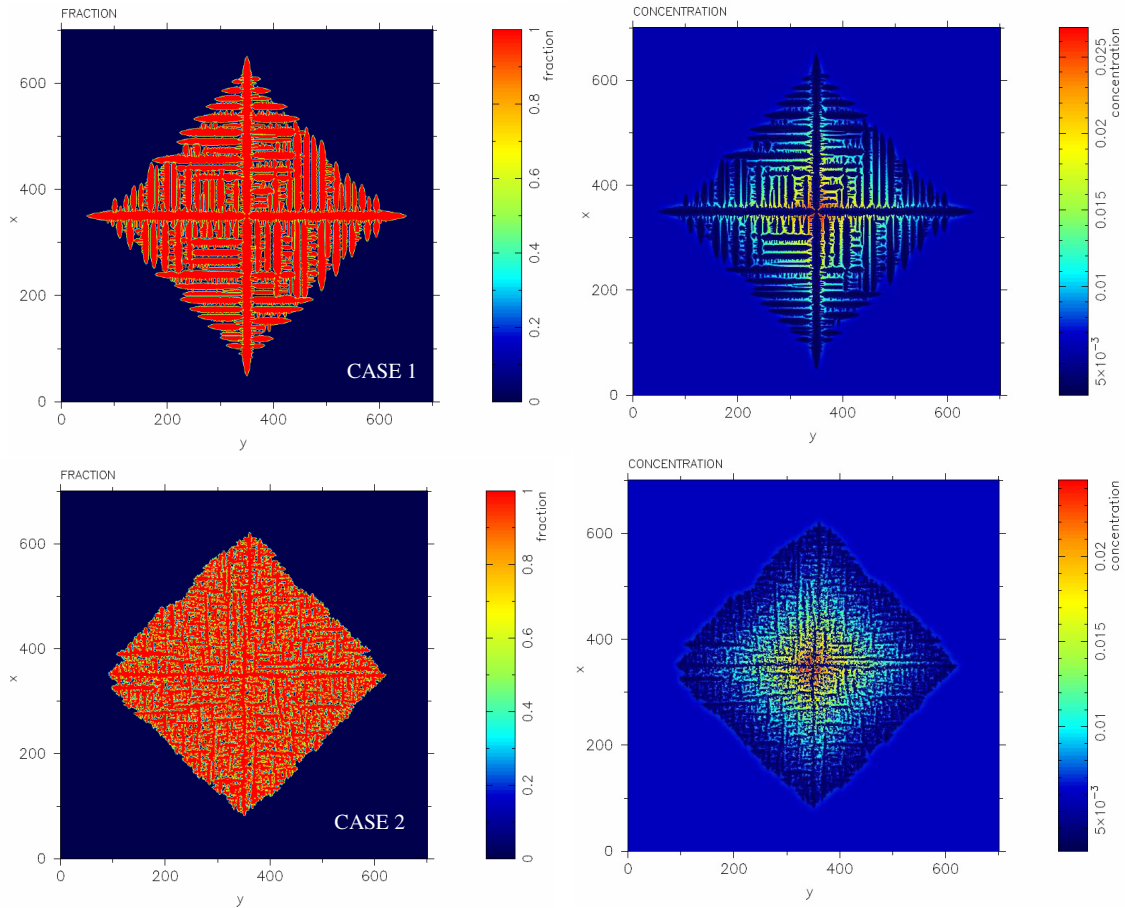


Figure 5: Solid fraction and concentration fields simulated by FDM-CA method (Case 1) and FDM-PA method (Case 2) for undercooling temperature $\Delta T = 250^\circ \text{C}$ after 0.76×10^{-5} [s]

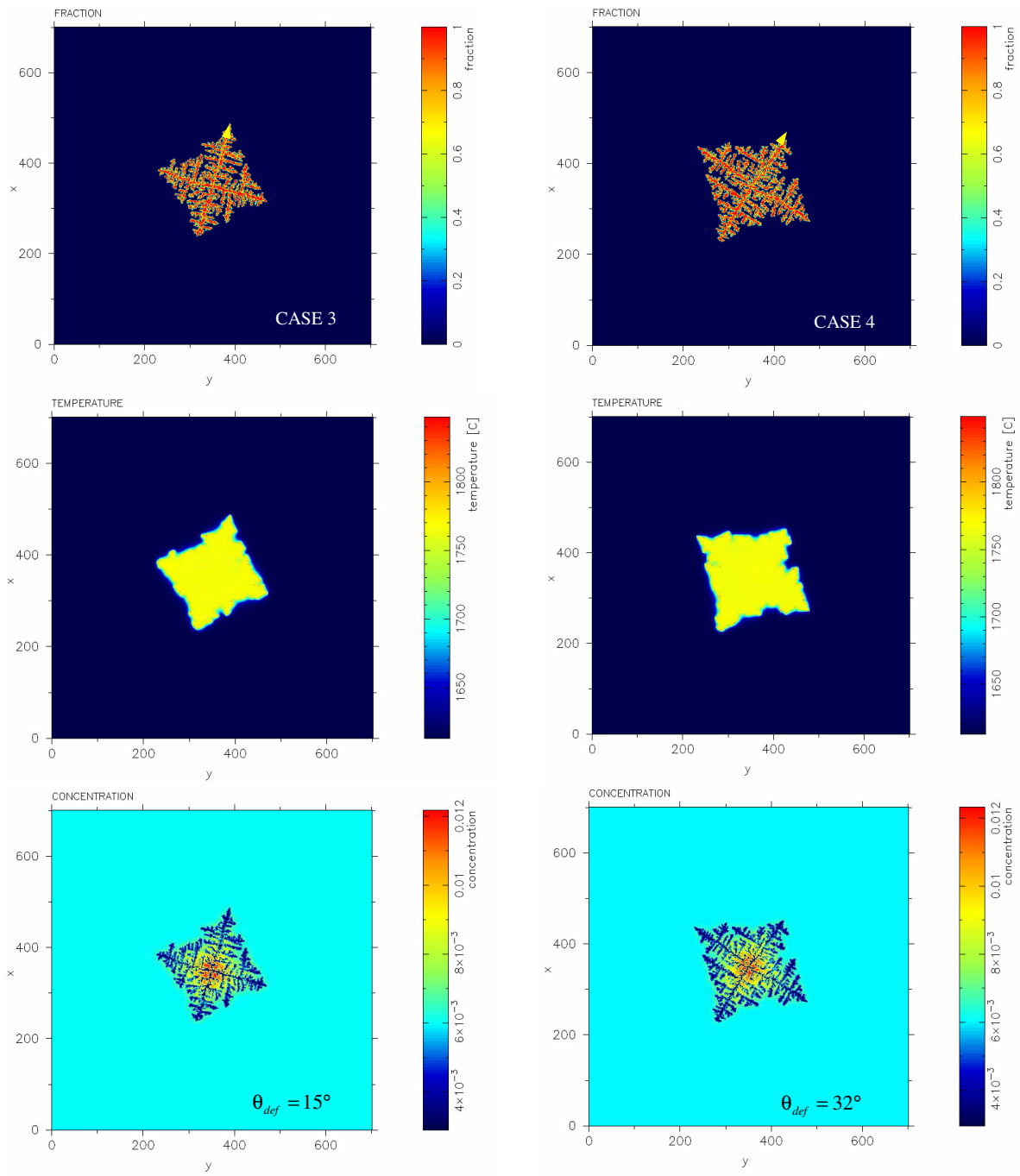


Figure 6: Solid fraction, temperature and concentration fields simulated by FDM-PA method for two different preferential orientations: Case 3 ($\theta_{def} = 15^\circ$) and Case 4 ($\theta_{def} = 32^\circ$) after 1.53×10^{-5} [s]

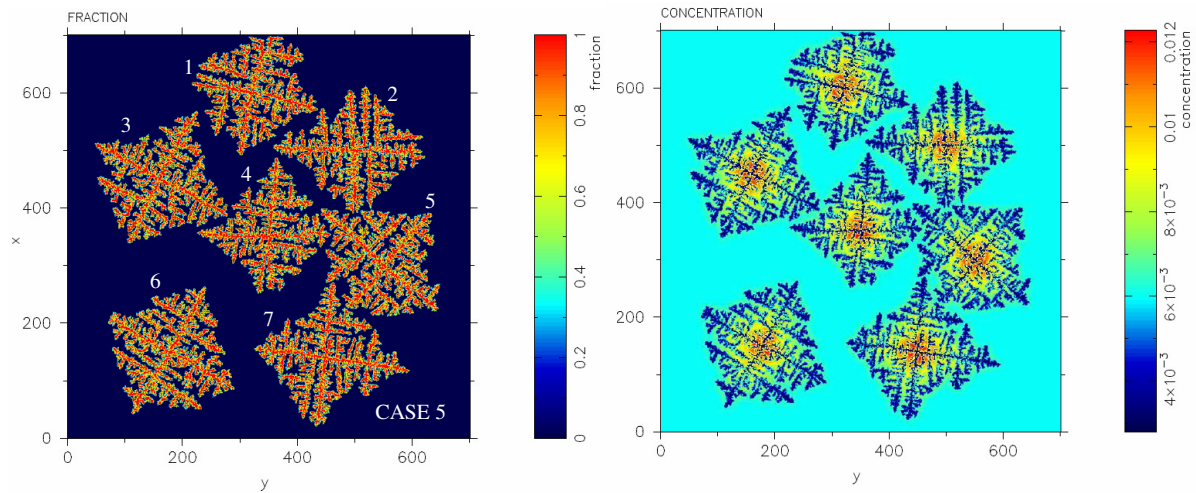


Figure 7: Seven dendrites growing simultaneously simulated by the FDM-PA method (Case 5) for 14° (1), 0° (2), 28° (3), 4° (4), 43° (5), 33° (6), 8° (7) preferred orientations after 1.53×10^{-5} [s]

- [3] Nastac, L. Modelling and Simulation of Microstructure Evolution in Solidifying Alloys. Kluwer Academic Publishers (2004).
- [4] Janssens, K.G.F. Three dimensional, space-time coupled cellular automata for the simulation of recrystallization and grain growth. *Modelling and Simulation in Materials Science and Engineering* (2003) **11**: 157-171.
- [5] Janssens, K.G.F. An introductory review of cellular automata modelling of moving grain boundaries in polycrystalline materials. *Mathematics and Computers in Simulations* (2010) **80**: 1361-1381.
- [6] Nastac, L. Numerical modeling of solidification and segregation patterns in cast alloys. *Acta Metallurgica* (1999) **47**: 4252-4262.
- [7] Daming, L., Ruo, L. and Zhang, P. A new coupled model for alloy solidification. *Science in China Ser. A. Mathematics* (2004) **47**: 41-52.
- [8] Zhu, M.Z., Dai, T., Lee, S.Y. and Hong, C.P. Modeling of solutal dendritic growth with melt convection. *Science Direct* (2008) **55**: 1620-1628.
- [9] Saito, Y., Goldbeck-Wood, G. and Muller-Krumbhaar, H. Numerical simulation of dendritic growth. *Physical Review* (1988) **33**: 2148-2157.
- [10] Zhu, M.F. and Hong, C.P. A modified cellular automata model for the simulation of dendritic growth in solidification of alloys. *ISIJ International* (2001) **5**: 436-445.
- [11] Sasikumar, R. and Sreenivasan, R. Two-dimensional simulation of dendrite morphology. *Acta metall. Mater* (1994) **42**: 2381-2386.
- [12] Voller, V.R. An enthalpy method for modelling dendritic growth in a binary alloy. *International Journal of Heat and Mass Transfer* (2008) **52**: 823-834.